JACS
JOURNAL OF THE AMERICAN CHEMICAL SOCIETY
Communication
pubs.acs.org/JACS

Lab-in-a-Shell: Encapsulating Metal Clusters for Size Sieving Catalysis

Zhen-An Qiao,[†] Pengfei Zhang,*[,†] Song-Hai Chai,[†] Miaofang Chi,[§] Gabriel M. Veith,[#] Nidia C. Gallego,[#] Michelle Kidder,[†] and Sheng Dai*[,†,‡]

[†]Chemical Sciences Division, [§]Center for Nanophase Material Sciences, and [#]Materials Science and Technology Division, Oak Ridge National Laboratory, Oak Ridge, Tennessee 37831, United States

[‡]Department of Chemistry, University of Tennessee, Knoxville, Tennessee 37996-1600, United States

Supporting Information

ABSTRACT: Here we describe a lab-in-a-shell strategy for the preparation of multifunctional core−shell nanospheres consisting of a core of metal clusters and an outer microporous silica shell. Various metal clusters (e.g., Pd and Pt) were encapsulated and confined in the void space mediated by the entrapped polymer dots inside hollow silica nanospheres acting first as complexing agent for metal ions and additionally as encapsulator for clusters, limiting growth and suppressing the sintering. The Pd clusters encapsulated in hybrid core−shell structures exhibit exceptional size-selective catalysis in allylic oxidations of substrates with the same reactive site but different molecular size (cyclohexene ∼0.5 nm, cholesteryl acetate ∼1.91 nm). The solvent-free aerobic oxidation of diverse hydrocarbons and alcohols was further carried out to illustrate the benefits of such an architecture in catalysis. High activity, outstanding thermal stability and good recyclability were observed over the core−shell nanocatalyst.

Metal catalysts are playing a vital role in petroleum refining, fine chemical production, and environmental protection, such as automobile exhaust treatment and selective oxidation.[1] In general, metal particles, typically with a size of 1−10 nm, are dispersed on support materials of high surface area to expose a high fraction of accessible atoms on the surface of the particles.[2] During the past few decades, extensive efforts have focused on the control of particle size of metals, the nature of the supports, and the surface and interfacial effects to improve the performance of these catalysts.[3] However, many intractable problems that hinder the development of this field (one of them is the thermally induced sintering) still remain.[4] The supported metal particles tend to grow or aggregate during the catalysis process, accompanied by a distinct loss of catalytic activity. Additionally, metal particles usually detach from the supports when the corresponding catalyst is rubbed reciprocally, which results in a sharp decrease of the activity. Hence the design of an ideal nanostructure for metal supported catalysts that can overcome the above-mentioned limits, at the same time displaying high stability, is a great challenge in this field.[5]

Encapsulation of metal particles into a nanoporous shell to form a core−shell nanostructure is a straightforward and effective strategy to address the problems of particle aggregation and detachment from the support.[6] One important role of this strategy is to hinder the interaction/contact between metal particles and thereby keep active metal cores stable even under harsh conditions, meanwhile allowing the smooth diffusion of small reactant molecules in and out of the shells. Moreover, the enclosed void space of core−shell nanoparticles is expected to be useful for chemical storage, compartmentation, and confinement of host−guest interactions in the catalysis processes.[7]

Several approaches have been developed for the synthesis of core−shell nanostructures, such as soft template, ship-in-a-bottle, Kirkendall effect, galvanic replacement, inside-out Ostwald ripening process, and so forth.[8] Although some progress in the synthesis of core−shell structures has been achieved, most of these methods still suffer from some disadvantages, such as low efficiency and tedious processing steps, which mainly result in a low yield. In addition, there are only a limited set of reports that can stabilize or entrap almost the smallest nanoparticle clusters (≤2 nm), with extremely high activity, into the interior of the hollow structures.[9]

Herein, we demonstrate a facile, efficient, yet unexplored approach, referred to as a lab-in-a-shell strategy, for the fabrication of a new type of core−shell nanospheres with a hollow microporous silica shell, encapsulating and immobilizing various metal clusters inside the cavity. The essence of the lab-in-a-shell strategy lies in the use of functionalized hollow shell as a microlaboratory integrating the laboratory functions and providing a unique microenvironment on a single hollow sphere of only several nanometers in size.[10] Our core−shell structured metal cluster@silica nanospheres were prepared by this approach in three steps (Figure 1a): (1) polymerization of ethylenediamine and carbon tetrachloride inside the hollow silica nanospheres to form polymer dot@silica core−shell nanoreactors;[11] (2) adsorbing and fixing target metal ions by the amine groups at the surface of polymer dots; and (3) H_2 in situ reduction of metal ions to metal clusters, removal of the polymers by calcination in the air and H_2 reduction of metal oxide to produce the metal cluster@silica core−shell nanospheres. As a result, the metal clusters were successfully encapsulated with both super-fine particle size (0.8−4.5 nm), which is much smaller than those of nanoparticles prepared by the conventional methods,[12] and uniform size distribution. In this approach, the polymer dot@silica core−shell structures

Received: June 12, 2014
Published: July 30, 2014

   dx.doi.org/10.1021/ja505903r | J. Am. Chem. Soc. 2014, 136, 11260−11263

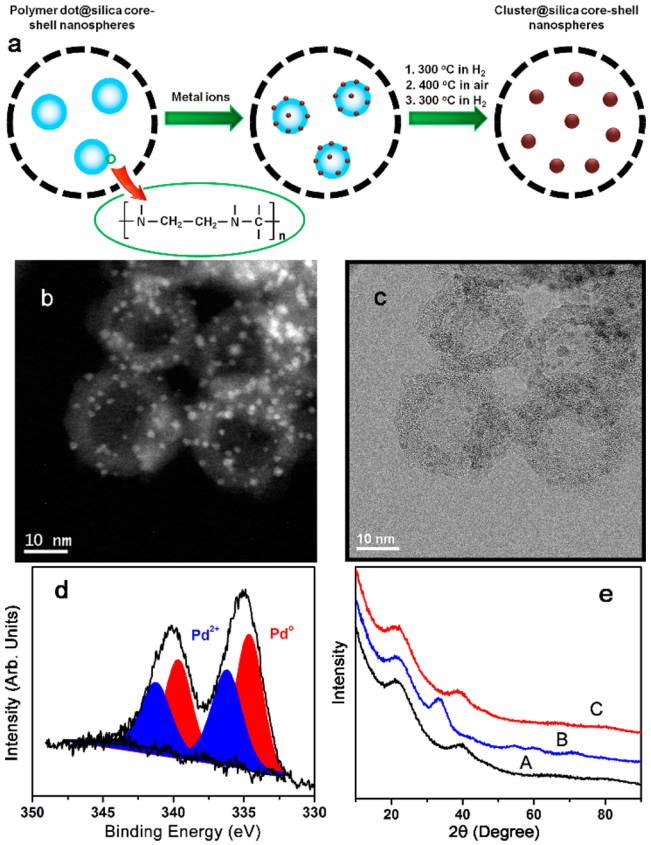

Figure 1. Procedure for the preparation of metal cluster@silica core–shell nanospheres (a). TEM images of Pd cluster@silica core–shell nanospheres: (b) *Z*-contrast and (c) bright-field. (d) Pd 3d XPS spectra for Pd cluster@silica nanospheres. (e) XRD patterns for Pd cluster/polymer@silica nanospheres (A), PdO cluster@silica nanospheres (B), and Pd cluster@silica nanospheres (C).

have a profound effect on the formation of the metal clusters. The large amount of residual amine groups on the polymer dots surface acts as a coordinating agent for the target metal ions and additionally as an encapsulator for the metal clusters, limiting growth and aggregation, especially when used at high temperature (up to 600 °C) in the synthesis.

Transmission electron microscopic (TEM) images of the as-prepared Pd cluster@silica core–shell nanospheres are presented in Figure 1. These images clearly reveal that Pd clusters are successfully encapsulated inside the silica hollow spheres, and most of the core clusters are attached on the interior wall of the silica shell due to the gravity. The entrapped Pd clusters have a narrow size distribution in the range of 1.1–2.3 nm as estimated from the TEM images (Figure 1b, c). Low-magnification TEM and elemental mapping images (Figure S1) show that the distribution of Pd clusters are evenly dispersed within the hollow silica nanospheres. The dispersion of 66.7% and particle size of 1.7 nm were also measured by pulse H_2 chemisorption of Pd in this sample. In addition, the amount of entrapped Pd clusters could be easily controlled from 0.1 to 15 wt % by adjusting the concentration of $PdCl_2$ precursor solution.

X-ray photoelectron spectroscopy (XPS) reveals that the Pd cluster@silica nanospheres exhibit two energy bands at 339.7 and 334.7 eV, which are typical values for the Pd $3d_{3/2}$ and $3d_{5/2}$ electrons of metallic Pd^0 (Figure 1d). The peaks around 336.3 and 341.3 eV correspond to Pd^{2+} species, suggesting that some of the Pd^0 surface atoms have been oxidized to Pd^{2+} by O_2 in the air, owing to their extremely high activity. The formation of Pd metallic clusters was also further confirmed by the wide-angle X-ray powder diffraction (XRD) pattern (Figure 1e). From the patterns of Pd cluster@silica nanospheres, only one broad Pd diffraction peaks can be seen at $2\theta = 38.15°$ assigned to (111) reflections of the cubic (fcc) palladium lattice (JCPDS no. 46-1043) as well as a very broad signal at $2\theta = 22.31°$ ascribed to amorphous silica, indicating the presence of ultrasmall crystalline Pd inside the hollow silica nanospheres. The average size of the Pd clusters is 1.6 nm calculated by the Scherrer equation, which is in agreement with the value obtained from TEM images. The FTIR spectrum of Pd cluster@silica spheres shows that the interior polymers have been completely burned off in the air (Figure S2). After calcinations in air at 400 °C for removal of the polymer, the Pd clusters were actually oxidized to obtain PdO clusters with a cluster size of 2.6 nm as shown by the XRD pattern. Interestingly, the entrapped Pd clusters are very stable. The size only increases from 1.6 to 2.5 nm as the temperature increasing from 300 to 600 °C in the H_2. These results indicate that the entrapped Pd clusters are prevented from sintering and aggregation even at a high reaction temperature.

The entrapment of Pt clusters was also confirmed by TEM and XPS (Figure 2). The size of Pt clusters assembled inside

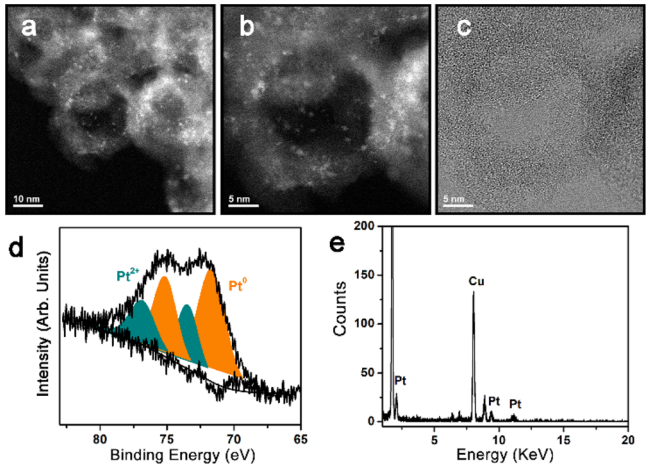

Figure 2. TEM images of Pt cluster@silica core–shell nanospheres: (a, b) *Z*-contrast and (c) bright field. Pt 4f XPS (d) and EDX (e) spectra for Pt cluster@silica nanospheres.

the silica spheres ranges from 10 to 50 atoms (Figure 2a–c). The diameter of ~0.8 nm was averaged from 100 randomly selected clusters. The Pt^0 $4f_{7/2}$ and $4f_{5/2}$ peaks are centered at 71.6 and 75.1 eV, while the peaks around 73.4 and 76.8 eV correspond to Pt^{2+} species, similar to the Pd samples (Figure 2d). No peaks of Pt^{4+} were observed, which suggested that all of Pt^{4+} precursor had been reduced in situ by H_2 treatment. The energy dispersive X-ray spectroscopy (EDX) spectrum of composite nanomaterials clearly identifies the peaks of element Pt (Figure 2e). Additionally, we could not observe any Pt and PtO_2 peaks in the XRD patterns synthesis (Figure S3). The size of entrapped Pt clusters can be readily controlled from 0.8 to 4.2 nm by varying the calcination temperature of 400–500 °C in the air (Figure S4).

Actually, core–shell structures are powerful platforms for confined nanocatalysis, especially an ideal matrixes for "dream"

dx.doi.org/10.1021/ja505903r | J. Am. Chem. Soc. 2014, 136, 11260–11263

size-selective catalysis, which is common in nature (e.g., size recognition in biological enzymes), yet seldom realized by heterogeneous organocatalysis.[13] Considering the molecular sieving capability of the microporous silica shell (Figure S5) and the ultrasmall size of entrapped Pd clusters, molecular-size recognition of our core−shell catalyst was probed by the allylic oxidations of cyclohexene versus cholesteryl acetate (CA), substrates with the same reactive site but different molecular size (cyclohexene ~0.5 nm, CA ~1.91 nm). For comparison, 25 nm solid silica nanoparticles loading 0.9 wt % Pd on their surface were synthesized by wetness impregnation method, and size of Pd particles was in the range of 4−8 nm (Figure S6). In the presence of this Pd/silica catalyst, cyclohexene and CA were oxidized in 60 min with 2-cyclohexen-1-one, 2-cyclohexenol, cyclohexene oxide, and 7-ketocholesteryl acetate as main products, giving the conversions of 23.1% and 9.8%, respectively (Figure 3). Generally, the metal nanoparticles

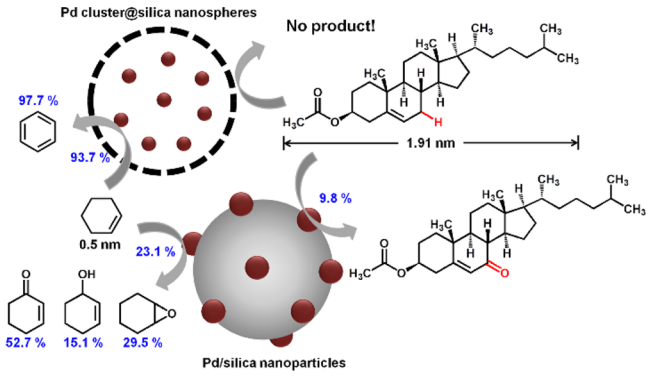

Figure 3. Size-selective catalysis of Pd cluster@silica core−shell nanospheres.

entrapped in the zeolite or MOF materials have a relatively low catalytic activity, because of large core particles prepared by traditional methods and slow mass diffusion through the thick microporous shells (hundreds of nanometers).[13] However, for our Pd cluster@silica catalyst (Pd loading of 0.9 wt %), around 4-fold cyclohexene conversion (93.7%) was reached with high selectivity for dehydrogenation product benzene (97.7%). The dehydrogenation of saturated C−C bond to C=C bond should be induced by the astonishingly fast hydride elimination of active Pd clusters, therefore suppressing the O_2-addition process (Supporting Information).[14] In sharp contrast, no detectable oxidation products of CA were observed by the Pd clusters−core@silica−shell catalyst. The size-sensitive performance of our core−shell catalyst can be directly ascribed to the molecular sieving characteristics of ultrathin microporous silica layer (~5 nm), which facilitates mass transfer of cyclohexene in liquid-phase oxidation but in turn lays a barrier between the big CA molecule and active Pd clusters inside (Supporting Information). The ultrasmall entrapped Pd clusters enable higher catalytic properties as compared to Pd nanoparticles synthesized by traditional approaches. The combination of the two factors results in the excellent size-selectivity and high catalytic activity of the core−shell catalyst.

The selective oxidation of organic compounds, such as hydrocarbons or alcohols, is a primary and essential transformation in organic synthesis and industrial chemistry.[15] The as-made core−shell nanospheres with multi unique characters in principle could also afford some exceptional performance, and therefore solvent-free oxidation of hydrocarbons or alcohols by atmospheric O_2 were studied over Pd cluster@silica nanospheres (Pd loading of 0.9 wt %). The core−shell nanocatalyst was very active for hydrocarbons (Table 1, entries

Table 1. Oxidation of Hydrocarbons and Alcohols Catalyzed by Pd Cluster@Silica Core−Shell Nanospheres[a]

	Substrate	Product (Sel. %)	T (°C)	TOF (h^{-1})[b]	Con. (%)
1		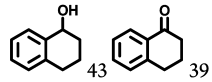 43 39	100	469	38.7 (8.0)[c]
2		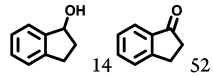 14 52	100	513	60.7
3	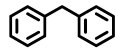	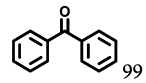 99	120	431	28.0
4		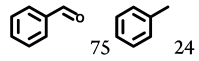 75 24	120	40910	29.8
5		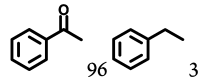 96 3	160	54740	26.5
6		 98	140	417	9.6
7		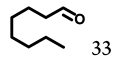 33 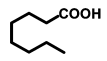 65	140	750	11.8

[a]Reaction conditions: hydrocarbon 4 mL or alkanol 4 mL or aromatic alcohol 40 mL, 0.9 wt % Pd cluster@silica 20 mg, O_2 1 atm, 20 h. [b]TOF = [reacted mol substrate]/[(total mol metal) × (reaction time)]. The TOFs were measured after 0.5 h of reaction. [c]Controlled oxidation without catalyst.

1−3), representative alcohols (entries 4−7) with remarkable turnover frequencies (tetralin, 469 h^{-1}; benzyl alcohol, 40910 h^{-1}). During the oxidation of chemically inert aliphatic octan-2-ol, a record TOF of 417 h^{-1} was achieved, which is significantly higher than previous results reported by other active catalysts, such as Au-Pd@TiO_2 (0 h^{-1}),[15a] Pd@N-Carbon (TOF: 86 h^{-1}),[15b] Pd@Hydroxyapatite (TOF: 7 h^{-1}),[1c] Ru(OH)x@Fe_3O_4 (TOF: 4 h^{-1}).[15c] Besides the high catalytic activity, the core−shell nanospheres also have a good thermal stability under high reduction temperature. The catalytic activity of Pd cluster@silica nanospheres was well retained after temperatures up to 600 °C under H_2 atmosphere, indicating that the morphology and cluster size are not essentially changed after the high-temperature treatment. The core−shell catalyst could be reused at least 20 times without any loss of activity for benzyl alcohol oxidation (120 °C, O_2 1 atm), and the corresponding turnover number was estimated to be ~280,000 (Figure S7). In consideration of catalytic results and the size of the Pd clusters after reusing 20 times, it is reasonable to confirm the fully recyclable character of current Pd catalyst, a prerequisite for industrial application. The outstanding catalytic performance of the core−shell catalyst in the aerobic oxidation demonstrates that the unique structure in deed endows the entrapped ultrasmall clusters with high catalytic activity, high thermal stability, and favorable reusability

dx.doi.org/10.1021/ja505903r | J. Am. Chem. Soc. 2014, 136, 11260−11263

during the heterogeneous catalysis, while the microporous shell around the encapsulated metal clusters allows the small size reactant to freely access to the encapsulated metal sites. Moreover, the protective microporous shells could prevent aggregation of the metal nanoparticles.

In conclusion, we have demonstrated a versatile lab-in-a-shell strategy to encapsulate various clusters within hollow silica nanospheres in a controllable way. This strategy is applicable to a broad range of clusters in non-agglomerated fashion and is capable of controlling the spatial distribution of clusters within the hollow silica matrix. On the basis of the characterization of their core−shell structure, the catalytic properties were explored in the solvent-free aerobic oxidation of hydrocarbons and alcohols, and the core−shell nanospheres were shown to have excellent catalytic activity with unexpected size selectivity, high thermal stability, and good recyclability. It is expected that such metal cluster@silica core−shell nanoreactors will serve as a useful platform to control substrate orientation and reactivity in heterogeneous catalysis as the diffusion of reactants and morphology of active catalysts can readily be manipulated through rational catalyst design. We believe the synthesis strategy reported here may open up new opportunities for preparing core−shell structured nanomaterials with various compositions.

■ ASSOCIATED CONTENT

Ⓢ Supporting Information

Experimental details and additional figures. This material is available free of charge via the Internet at http://pubs.acs.org.

■ AUTHOR INFORMATION

Corresponding Author

dais@ornl.gov; chemistryzpf@163.com

Notes

The authors declare no competing financial interest.

■ ACKNOWLEDGMENTS

This work was supported by the U.S. Department of Energy, Office of Science, Basic Energy Sciences, Chemical Sciences, Geosciences, and Biosciences Division. A portion of this research was conducted at the Center for Nanophase Materials Sciences, which is sponsored at Oak Ridge National Laboratory by the Division of Scientific User Facilities, Office of Basic Energy Sciences, U.S.

■ REFERENCES

(1) (a) Abad, A.; Concepcion, P.; Corma, A.; Garcia, H. *Angew. Chem., Int. Ed.* **2005**, *44*, 4066. (b) Kesavan, L.; Tiruvalam, R.; Ab Rahim, M. H.; bin Saiman, M. I.; Enache, D. I.; Jenkins, R. L.; Dimitratos, N.; Lopez-Sanchez, J. A.; Taylor, S. H.; Knight, D. W.; Kiely, C. J.; Hutchings, G. J. *Science* **2011**, *331*, 195. (c) Mori, K.; Hara, T.; Mizugaki, T.; Ebitani, K.; Kaneda, K. *J. Am. Chem. Soc.* **2004**, *126*, 10657.

(2) (a) Bell, A. T. *Science* **2003**, *299*, 1688. (b) Zheng, N. F.; Stucky, G. D. *J. Am. Chem. Soc.* **2006**, *128*, 14278. (c) Corma, A. *Chem. Rev.* **1997**, *97*, 2373.

(3) (a) Chen, C.; Nan, C. Y.; Wang, D. S.; Su, Q. A.; Duan, H. H.; Liu, X. W.; Zhang, L. S.; Chu, D. R.; Song, W. G.; Peng, Q.; Li, Y. D. *Angew. Chem., Int. Ed.* **2011**, *50*, 3725. (b) Do, P. T. M.; Foster, A. J.; Chen, J. G.; Lobo, R. F. *Green Chem.* **2012**, *14*, 1388.

(4) (a) Joo, S. H.; Park, J. Y.; Tsung, C. K.; Yamada, Y.; Yang, P. D.; Somorjai, G. A. *Nat. Mater.* **2009**, *8*, 126. (b) Datta, K. K. R.; Reddy, B. V. S.; Ariga, K.; Vinu, A. *Angew. Chem., Int. Ed.* **2010**, *49*, 5961.

(5) (a) Lu, J. L.; Fu, B. S.; Kung, M. C.; Xiao, G. M.; Elam, J. W.; Kung, H. H.; Stair, P. C. *Science* **2012**, *335*, 1205. (b) Chan-Thaw, C. E.; Villa, A.; Katekomol, P.; Su, D. S.; Thomas, A.; Prati, L. *Nano Lett.* **2010**, *10*, 537.

(6) (a) Arnal, P. M.; Comotti, M.; Schuth, F. *Angew. Chem., Int. Ed.* **2006**, *45*, 8224. (b) Liu, J.; Yang, H. Q.; Kleitz, F.; Chen, Z. G.; Yang, T. Y.; Strounina, E.; Lu, G. Q.; Qiao, S. Z. *Adv. Funct. Mater.* **2012**, *22*, 591. (c) Huang, X. Q.; Tang, S. H.; Liu, B. J.; Ren, B.; Zheng, N. F. *Adv. Mater.* **2011**, *23*, 3420.

(7) Liu, R.; Mahurin, S. M.; Li, C.; Unocic, R. R.; Idrobo, J. C.; Gao, H. J.; Pennycook, S. J.; Dai, S. *Angew. Chem., Int. Ed.* **2011**, *50*, 6799.

(8) (a) Liu, J.; Qiao, S. Z.; Hartono, S. B.; Lu, G. Q. *Angew. Chem., Int. Ed.* **2010**, *49*, 4981. (b) Yin, Y. D.; Rioux, R. M.; Erdonmez, C. K.; Hughes, S.; Somorjai, G. A.; Alivisatos, A. P. *Science* **2004**, *304*, 711. (c) Liu, J.; Qiao, S. Z.; Chen, J. S.; Lou, X. W.; Xing, X. R.; Lu, G. Q. *Chem. Commun.* **2011**, *47*, 12578.

(9) (a) Nie, X. T.; Qian, H. F.; Ge, Q. J.; Xu, H. Y.; Jin, R. C. *ACS Nano* **2012**, *6*, 6014. (b) Ma, G. C.; Binder, A.; Chi, M. F.; Liu, C.; Jin, R. C.; Jiang, D. E.; Fan, J.; Dai, S. *Chem. Commun.* **2012**, *48*, 11413.

(10) (a) Duan, R. X.; Zuo, X. L.; Wang, S. T.; Quan, X. Y.; Chen, D. L.; Chen, Z. F.; Jiang, L.; Fan, C. H.; Xia, F. *J. Am. Chem. Soc.* **2013**, *135*, 4604. (b) Schmit, V. L.; Martoglio, R.; Scott, B.; Strickland, A. D.; Carron, K. T. *J. Am. Chem. Soc.* **2012**, *134*, 59.

(11) Qiao, Z. A.; Huo, Q. S.; Chi, M. F.; Veith, G. M.; Binder, A. J.; Dai, S. *Adv. Mater.* **2012**, *24*, 6017.

(12) (a) Schalow, T.; Brandt, B.; Starr, D. E.; Laurin, M.; Shaikhutdinov, S. K.; Schauermann, S.; Libuda, J.; Freund, H. J. *Angew. Chem., Int. Ed.* **2006**, *45*, 3693. (b) Davis, S. E.; Ide, M. S.; Davis, R. J. *Green Chem.* **2013**, *15*, 17. (c) Johnston, E. V.; Verho, O.; Karkas, M. D.; Shakeri, M.; Tai, C. W.; Palmgren, P.; Eriksson, K.; Oscarsson, S.; Backvall, J. E. *Chem.—Eur. J.* **2012**, *18*, 12202.

(13) (a) Lu, G.; Li, S. Z.; Guo, Z.; Farha, O. K.; Hauser, B. G.; Qi, X. Y.; Wang, Y.; Wang, X.; Han, S. Y.; Liu, X. G.; DuChene, J. S.; Zhang, H.; Zhang, Q. C.; Chen, X. D.; Ma, J.; Loo, S. C. J.; Wei, W. D.; Yang, Y. H.; Hupp, J. T.; Huo, F. W. *Nat. Chem.* **2012**, *4*, 310. (b) Shang, Z. Y.; Patel, R. L.; Evanko, B. W.; Liang, X. H. *Chem. Commun.* **2013**, *49*, 10067. (c) Rajagopalan, R.; Ponnaiyan, A.; Mankidy, P. J.; Brooks, A. W.; Yi, B.; Foley, H. C. *Chem. Commun.* **2004**, 2498.

(14) Campbell, A. N.; Stahl, S. S. *Acc. Chem. Res.* **2012**, *45*, 851.

(15) (a) Enache, D. I.; Edwards, J. K.; Landon, P.; Solsona-Espriu, B.; Carley, A. F.; Herzing, A. A.; Watanabe, M.; Kiely, C. J.; Knight, D. W.; Hutchings, G. J. *Science* **2006**, *311*, 362. (b) Zhang, P. F.; Gong, Y. T.; Li, H. R.; Chen, Z. R.; Wang, Y. *Nat. Commun.* **2013**, *4*, 1593. (c) Kotani, M.; Koike, T.; Yamaguchia, K.; Mizuno, N. *Green Chem.* **2006**, *8*, 735. (d) Prati, L.; Porta, F.; Wang, D.; Villa, A. *Catal. Sci. Technol.* **2011**, *1*, 1624. (e) Chen, Y.; Wang, H.; Liu, C.; Zeng, Z.; Zhang, H.; Zhou, C.; Jia, X.; Yang, Y. *J. Catal.* **2012**, *289*, 105.